Improved accuracy of cortical bone mineralization measured by polychromatic microcomputed tomography using a novel high mineral density composite calibration phantom

Justin M. Deuerling, David J. Rudy, Glen L. Niebur, and Ryan K. Roeder[a)]
Department of Aerospace and Mechanical Engineering, University of Notre Dame, Notre Dame, Indiana 46556

(Received 12 April 2010; revised 22 July 2010; accepted for publication 22 July 2010; published 31 August 2010)

Purpose: Microcomputed tomography (micro-CT) is increasingly used as a nondestructive alternative to ashing for measuring bone mineral content. Phantoms are utilized to calibrate the measured x-ray attenuation to discrete levels of mineral density, typically including levels up to 1000 mg HA/cm^3, which encompasses levels of bone mineral density (BMD) observed in trabecular bone. However, levels of BMD observed in cortical bone and levels of tissue mineral density (TMD) in both cortical and trabecular bone typically exceed 1000 mg HA/cm^3, requiring extrapolation of the calibration regression, which may result in error. Therefore, the objectives of this study were to investigate (1) the relationship between x-ray attenuation and an expanded range of hydroxyapatite (HA) density in a less attenuating polymer matrix and (2) the effects of the calibration on the accuracy of subsequent measurements of mineralization in human cortical bone specimens.
Methods: A novel HA-polymer composite phantom was prepared comprising a less attenuating polymer phase (polyethylene) and an expanded range of HA density (0–1860 mg HA/cm^3) inclusive of characteristic levels of BMD in cortical bone or TMD in cortical and trabecular bone. The BMD and TMD of cortical bone specimens measured using the new HA-polymer calibration phantom were compared to measurements using a conventional HA-polymer phantom comprising 0–800 mg HA/cm^3 and the corresponding ash density measurements on the same specimens.
Results: The HA-polymer composite phantom exhibited a nonlinear relationship between x-ray attenuation and HA density, rather than the linear relationship typically employed *a priori*, and obviated the need for extrapolation, when calibrating the measured x-ray attenuation to high levels of mineral density. The BMD and TMD of cortical bone specimens measured using the conventional phantom was significantly lower than the measured ash density by 19% ($p<0.001$, ANCOVA) and 33% ($p<0.05$, Tukey's HSD), on average, respectively. The BMD and TMD of cortical bone specimens measured using the HA-polymer phantom with an expanded range of HA density was significantly lower than the measured ash density by 8% ($p<0.001$, ANCOVA) and 10% ($p<0.05$, Tukey's HSD), on average, respectively.
Conclusions: The new HA-polymer calibration phantom with a less attenuating polymer and an expanded range of HA density resulted in a more accurate measurement of micro-CT equivalent BMD and TMD in human cortical bone specimens compared to a conventional phantom, as verified by ash density measurements on the same specimens. [DOI: 10.1118/1.3480507]

Key words: bone mineral density, cortical bone, hydroxyapatite, microcomputed tomography, mineralization

I. INTRODUCTION

The level of mineralization is an important determinant of the mechanical properties and fracture susceptibility of bone tissue.[1] Cortical bone mechanical properties—such as the elastic modulus, strength, and fracture toughness—are strongly influenced by mineralization.[2–6] Moreover, a parametric study using a multiscale, micromechanical model demonstrated that the elastic modulus of cortical bone was most sensitive to the mineral density, among seven structural parameters investigated.[7] Therefore, precise and reliable techniques are needed for measuring the level of mineralization in bone tissue.

Mineralization is most commonly and accurately measured by ashing bone tissue at a temperature sufficient to pyrolyze the organic matrix, leaving the bone mineral for gravimetric analysis. Unfortunately, this process is inherently invasive and destructive. Mineralization has also been measured using backscattered electron imaging in a scanning electron microscope[8,9] and microradiography.[9,10] These techniques are capable of very fine spatial resolution but are inherently invasive and two-dimensional. In contrast, peripheral quantitative computed tomography (pQCT) has enabled noninvasive, three-dimensional (3D) measurement of volumetric bone mineral density (BMD) but has a relatively low spatial resolution for examining levels of mineralization.[11]

Synchrotron radiation computed tomography (SRCT) is capable of precise, 3D measurements of bone mineralization[9,12,13] but is limited in availability and to a small specimen size.

Therefore, microcomputed tomography (micro-CT) has been proposed for nondestructive, 3D measurements of bone mineralization using a linear calibration of mineral density and x-ray attenuation.[13–20] Both micro-CT and SRCT have sufficient spatial resolution to enable volumetric measurement of tissue mineral density (TMD), exclusive of porosity, in addition to BMD, inclusive of porosity.[13,14] However, measurements of mineral density by micro-CT are complicated by beam hardening due to the use of polychromatic radiation. Beam hardening leads to an underestimation of x-ray attenuation, and subsequently mineral density, because the mean x-ray energy is higher for the specimen interior due to the preferential attenuation of low energy x rays at the specimen perimeter. Beam hardening correction algorithms are one approach used to mitigate this phenomenon, but may not be sufficient, especially at high levels of mineral density.[13–16]

Mixtures of polymers with known quantities of hydroxyapatite (HA) crystals are commonly used in micro-CT imaging phantoms for the calibration of x-ray attenuation to HA density.[13,14,17] Phantoms comprising HA are desirable because HA exhibits similar composition and x-ray attenuation compared to bone mineral. The measured x-ray attenuation versus the known HA density in the phantom is fitted by least-squares linear regression and this calibration is subsequently used to estimate the mineral density of bone specimens from the measured x-ray attenuation. Previous studies demonstrated strong correlations between micro-CT equivalent density and ash density measurements in trabecular and cortical bone; however, micro-CT underestimated TMD compared to the ash density.[13,14] Aqueous solutions containing varying concentrations of potassium phosphate (K_2HPO_4) have also been used as a micro-CT calibration phantom.[12,16,17,20] K_2HPO_4 was utilized due to exhibiting x-ray attenuation similar to HA and homogeneity throughout the liquid phantom.

Current HA-polymer and liquid K_2HPO_4 calibration phantoms share a common limitation. The range of mineral density commonly present in either HA-polymer composite (0–800 mg HA/cm^3) (Refs. 13, 14, and 17) or K_2HPO_4 solution (0–1000 mg HA/cm^3) (Refs. 12, 16, 17, and 20) phantoms encompasses levels of BMD observed in trabecular bone. However, levels of BMD observed in cortical bone and levels of TMD in cortical or trabecular bone typically exceed 1000 mg HA/cm^3, requiring extrapolation of linear calibration regressions.[13–16] Moreover, a nonlinear relationship between measured x-ray attenuation and known phantom mineral density has been observed even after the use of a beam hardening correction algorithm.[16] The presence of a nonlinear calibration of measured x-ray attenuation and known phantom mineral density suggests that the use of an extrapolated linear calibration would result in increased underestimation of the mineral density in tissue specimens at high levels of mineral density, as has been observed in practice.[13,14]

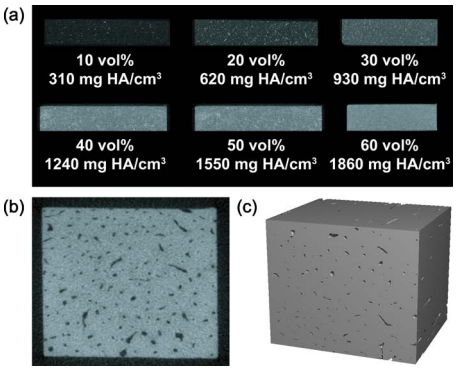

FIG. 1. Representative cross-sectional grayscale images for micro-CT of (a) the HA-polymer composite phantom showing increased brightness with increased HA density, as expected, and (b) a representative cortical bone specimen including (c) a segmented, three-dimensional reconstruction of the entire tissue specimen. Note that the vertical dimension of the phantom specimens in (a) is 2.5 mm, and the horizontal dimension of the tissue specimen in (b) and (c) is 5 mm.

Therefore, the objectives of this study were to investigate (1) the relationship between x-ray attenuation and an expanded range of HA density (0–1860 mg HA/cm^3) using a calibration phantom comprising 0–60 vol % HA crystals in a less attenuating polymer matrix and (2) the effects of the calibration on the accuracy of subsequent measurements of mineralization in human cortical bone specimens. The BMD and TMD of cortical bone specimens measured using the new HA-polymer calibration phantom were compared to measurements using a conventional HA-polymer phantom comprising 0–800 mg HA/cm^3 and the corresponding ash density measurements on the same specimens.

II. MATERIALS AND METHODS

II.A. Calibration phantoms

HA reinforced high density polyethylene (HDPE) composites composed of 0, 10, 20, 30, 40, 50, and 60 vol % HA were prepared using methods described in detail elsewhere.[21,22] The HA densities of the composites were calculated to be 0, 310, 620, 930, 1240, 1550, and 1860 mg HA/cm^3 [Fig. 1(a), Table I], based on the known density of HDPE (960 mg/cm^3) (Ref. 21) and HA crystals prepared using similar methods (3100 mg/cm^3).[23,24] The HA content in the composites was also verified using measurements from Archimedes' principle[25] and ashing.[22]

Composite bars with cross-sectional dimensions of 10 $\times$ 2.5 mm were each positioned near the outer edge of a 20 mm diameter specimen holder such that the specimen was within 7–10 mm from the center of rotation and scanned individually using a benchtop micro-CT system (μCT-80, Scanco Medical AG, Brüttisellen, Switzerland) equipped with a cone beam polychromatic x-ray source, 0.5 mm aluminum filter, and 2048 $\times$ 128 element charge-coupled device detector. Imaging was performed in de-ionized (DI) water

TABLE I. The new HA-polymer composite phantom with an expanded range of HA density encompassed levels of BMD characteristic of human cortical bone, and levels of TMD characteristic of both human cortical and trabecular bone. Measurements of the micro-CT equivalent mineral density for compositions of the new HA-polymer phantom using extrapolated linear or nonlinear calibrations for the conventional phantom (Fig. 2) significantly underestimated the known HA density ($p<0.01$, paired t-test). The first standard deviation of mean values is given in parentheses, when applicable, and represents intrascan spatial variability for a single volume of interest.

HA-polymer phantom composition		Micro-CT measurements		
HA volume fraction (vol %)	HA density (mg HA/cm^3)	X-ray attenuation (cm^{-1})	Linear calibrated equivalent density[a] (mg HA/cm^3)	Nonlinear calibrated equivalent density[b] (mg HA/cm^3)
0	0	0.24(0.18)	−97 (68)	−72 (58)
10	310	1.05(0.39)	215 (151)	208 (127)
20	620	1.72(0.58)	475 (225)	464 (191)
30	930	2.34(0.52)	714 (201)	718 (171)
40	1240	2.88(0.53)	925 (214)	958 (174)
50	1550	3.40(0.53)	1124 (204)	1196 (174)
60	1860	3.88(0.56)	1310 (218)	1430 (184)

[a]Measured using an extrapolated linear calibration for the conventional phantom.
[b]Measured using an extrapolated nonlinear calibration for the conventional phantom.

soaked gauze at 70 kVp, 114 μA, and 400 ms integration time for 200 slices with a 10 μm voxel size. All parameters known to affect x-ray attenuation measurements—such as the tube voltage, detector distance, detector size, and imaging media[17]—were held constant. A beam hardening correction algorithm based on a HA-resin wedge phantom (1200 mg HA/cm^3) was applied as provided by the micro-CT manufacturer. Analysis was conducted on a volume of interest, with boundaries reduced from the specimen outline by 50 pixels (0.5 mm) to remove partial volume artifacts, after applying a Gaussian filter (sigma=0.8, support =1.0) to minimize high frequency noise.

A conventional calibration phantom (QRM-microCT-HA, Quality Assurance in Radiology and Medicine, GmbH, Möhrendorf, Germany) provided by the micro-CT manufacturer comprised HA particles embedded in a proprietary epoxy resin (1130 mg/cm^3) at 0, 100, 200, 400, and 800 mg HA/cm^3 (Table II). All five HA compositions were embedded within a single, 35 mm diameter cylindrical block of the same epoxy resin, evenly spaced and centered about a 20 mm diameter from the center of rotation, and each individual HA composition was 6 mm in diameter. The conventional calibration phantom was scanned using identical methods to the HA-polymer phantom, except that the size of the conventional phantom necessitated lower resolution (18 μm voxel size) and each HA composition could not be scanned individually. Therefore, in order to consider the effects of the lower resolution and specimen positioning, the HA-polymer phantom compositions were also rescanned with an 18 μm voxel size either simultaneously (in parallel) or individually (in series) while placed the same distance from the center of rotation as the conventional phantom compositions.

Linear and nonlinear least-squares regression (STATVIEW 5.0.1, SAS Institute, Inc., Cary, NC) was used to correlate the measured x-ray attenuation with the known HA density in the calibration phantoms. Analysis of covariance (ANCOVA) was used to compare regressions. The known HA density within calibration phantoms was compared to the HA density determined from the measured x-ray attenuation and the calibration provided for the conventional phantom using a paired t-test. The level of significance for all tests was set at 0.05.

II.B. Measurements of cortical bone mineralization

Thirty-seven cortical bone specimens, nominally 5×5×5 mm, were machined from the femoral diaphysis of three human male donors ages 62, 62, and 70, presenting no medical history of skeletal pathology or trauma. All tissues were obtained with donor's consent (National Disease Research Interchange, Philadelphia, PA) and all protocols were approved by the Notre Dame Human Subjects Institutional Review Board. The entire volume of each specimen was scanned by micro-CT [Figs. 1(b) and 1(c)] in DI water soaked gauze using the same methods and parameters described above for the calibration phantoms. X-ray attenua-

TABLE II. The conventional phantom provided by the micro-CT manufacturer comprised a range of HA density that encompassed levels of BMD characteristic of human trabecular bone only. Repeated measurements of the micro-CT equivalent mineral density for compositions of the phantom using the linear calibration were not statistically different than the HA density quoted by the phantom manufacturer ($p>0.10$, paired t-test). The first standard deviation of mean values is given in parentheses, when applicable, and represents intrascan spatial variability for a single volume of interest.

Conventional phantom composition	Micro-CT measurements	
HA density[a] (mg HA/cm^3)	X-ray attenuation (cm^{-1})	Equivalent density[b] (mg HA/cm^3)
0	0.44(0.09)	−22 (34)
100	0.73(0.18	94 (69)
200	1.00(0.21)	198 (82)
400	1.51(0.24)	396 (91)
800	2.45(0.23)	760 (88)

[a]Provided by the phantom manufacturer.
[b]Repeated measurement using the linear calibration for the conventional phantom.

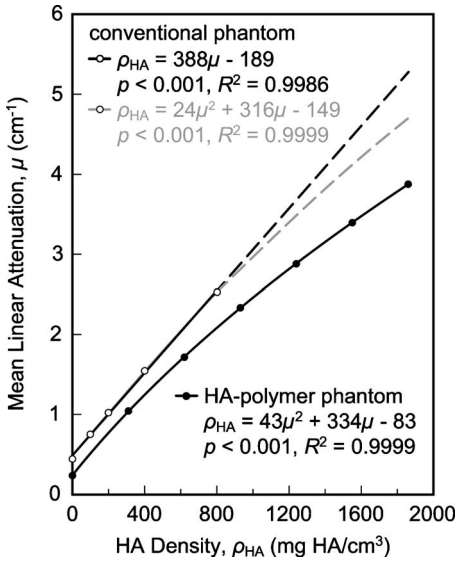

FIG. 2. The HA-polymer composite phantom with an expanded range of HA density exhibited a nonlinear relationship between the measured x-ray attenuation μ and the known HA density ρ_{HA}. The conventional phantom was fitted by a linear or a nonlinear relationship at the lower levels of HA density employed and extrapolated for higher levels of HA density. Therefore, calibration using the new HA-polymer phantom resulted in measurements of HA density that were significantly greater than those using extrapolated linear or nonlinear calibrations for the conventional phantom ($p<0.01$, paired t-test) (Table I), and the differences became greater with increased HA density.

tion was evaluated over either the total volume (TV), inclusive of porosity, or bone volume (BV), exclusive of porosity. Tissue porosity was segmented from the BV using a global threshold value of 240 on the grayscale images for all specimens. This threshold was located at the toe of the bone peak in the image histogram and corresponded to an x-ray attenuation of 1.92 cm^{-1} or 553 mg HA/cm^3 using the conventional calibration phantom provided by the manufacturer. The mean (±standard deviation) Haversian porosity measured by micro-CT for the cortical bone specimens investigated in this study was 10.1 (±7.1) vol %. BMD and TMD were measured based on the TV and BV, respectively, using linear and nonlinear calibrations of measured x-ray attenuation and known mineral density from the calibration phantoms (Fig. 2).

The ash density for each specimen was measured as the ash mass divided by either the TV or BV, for comparison to micro-CT measurements of BMD or TMD, respectively. TV was measured using Archimedes' principle as the difference between the specimen mass when fully saturated with DI water (M) and the apparent mass when suspended in DI water (S).[7,25,26] Each specimen was subsequently dehydrated in a graded series of alcohol solutions and dried in a vacuum oven at 100 °C for 24 h. BV was also measured using Archimedes' principle as the difference between the dry specimen mass (D) and S.[7,25,27] Specimens were finally ashed at 900 °C for 48 h. The ash mass, as well as the above measures of specimen mass, was measured gravimetrically to a precision of 0.1 mg. Measured ash densities were compared to measured micro-CT equivalent densities using ANCOVA (STATVIEW 5.0.1, SAS Institute, Inc., Cary, NC) or Tukey's HSD test, with a level of significance of 0.05.

III. RESULTS

III.A. Calibration phantoms

The HA-polymer composite phantom with an expanded range of HA density exhibited a nonlinear relationship between x-ray attenuation and HA density (Fig. 2). In contrast, the relationship between x-ray attenuation and HA density for the conventional phantom could be fitted by either a linear or a nonlinear relationship within the range of HA density in the phantom. Significant differences between the linear and nonlinear regressions were only observed upon extrapolation to HA density greater than the 800 mg HA/cm^3 upper limit of the phantom.

The HA-polymer phantom with an expanded range of HA density also utilized a lower density polymer that resulted in a significantly lower x-ray attenuation at any given HA density compared to the conventional phantom (Fig. 2). Therefore, calibration using the new HA-polymer phantom resulted in measurements of HA density that were significantly greater than those using extrapolated linear or nonlinear calibrations for the conventional phantom ($p<0.01$, paired t-test) (Table I), and the differences became greater with increased HA density (Fig. 2).

The HA-polymer composite and conventional calibration phantoms in Fig. 2 were imaged with a 10 versus 18 μm voxel size and with the various HA compositions imaged individually (in series) versus simultaneously (in parallel), respectively, due to the size and design of the commercial phantom. In order to consider these effects, the HA-polymer phantom compositions were also rescanned with an 18 μm voxel size either individually (in series) or simultaneously (in parallel) while placed the same distance from the center of rotation as the conventional phantom compositions. The lower resolution and simultaneous imaging of the HA-polymer composite specimens resulted in increased measured x-ray attenuation for a given HA density, but the differences from conditions employed in Fig. 2 were not statistically significant ($p=0.12$, ANCOVA) and the calibration remained nonlinear (Fig. 3). Therefore, subsequent measurements of cortical bone mineralization focused on the nonlinear calibration with HA-polymer composite phantom compositions imaged individually (in series) at the higher resolution (Fig. 2) in order to be most similar to the imaging methods employed for bone tissue specimens.

III.B. Measurements of cortical bone mineralization

The BMD of human cortical bone specimens measured by micro-CT was in closer agreement with the corresponding ash density using the nonlinear calibration for the HA-polymer phantom with an expanded range of HA density compared to extrapolated linear or nonlinear calibrations for the conventional phantom (Fig. 4). BMD measured using extrapolated linear or nonlinear calibrations for the conventional phantom was significantly lower than the measured

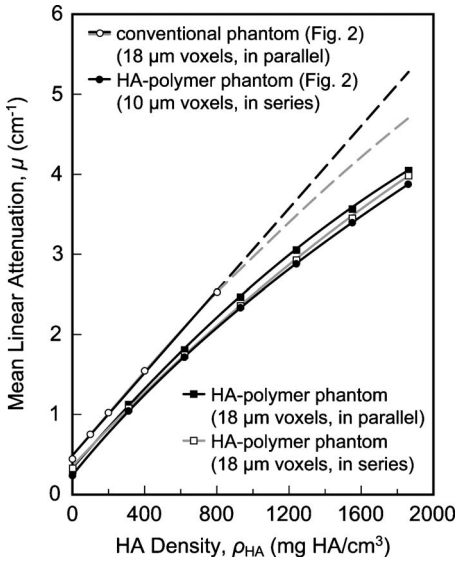

FIG. 3. The HA-polymer composite and conventional calibration phantoms in Fig. 2 were imaged with a 10 versus 18 μm voxel size, and with the various HA compositions imaged individually (in series) versus simultaneously (in parallel), respectively, due to the size and design of the commercial phantom. In order to consider these effects, the HA-polymer phantom compositions were also rescanned with an 18 μm voxel size either simultaneously (in parallel) or individually (in series) while placed the same distance from the center of rotation as the conventional phantom compositions. The lower resolution and simultaneous imaging of the HA-polymer composite specimens resulted in increased measured x-ray attenuation μ for a given HA density ρ_{HA}, but the differences from conditions employed in Fig. 2 were not statistically significant ($p=0.12$, ANCOVA) and the calibration remained nonlinear.

ash density ($p<0.001$, ANCOVA) by 19% or 17%, on average, respectively. BMD measured using the HA-polymer phantom with an expanded range of HA density was significantly greater than the measured ash density ($p<0.001$, ANCOVA) by 8%, on average. Micro-CT measurements of BMD were correlated with ash density measurements using both the nonlinear calibration for the HA-polymer composite phantom ($p<0.001$, $R^2=0.55$) and extrapolated linear or nonlinear calibrations with the conventional phantom ($p<0.001$, $R^2=0.56$).

The TMD of human cortical bone specimens measured by micro-CT was also in closer agreement with the corresponding ash density using the nonlinear calibration for the HA-polymer composite phantom with an expanded range of HA density compared to extrapolated linear or nonlinear calibrations for the conventional phantom (Fig. 5). Micro-CT measurements of TMD using either calibration phantom were not correlated with ash density measurements ($p>0.66$). However, TMD measured using extrapolated linear or nonlinear calibrations for the conventional phantom underestimated the ash density by 33% or 30%, on average, respectively, while TMD measured using the nonlinear calibration for the HA-polymer phantom underestimated the ash density by only 10%, on average ($p<0.05$, Tukey's HSD) (Fig. 6).

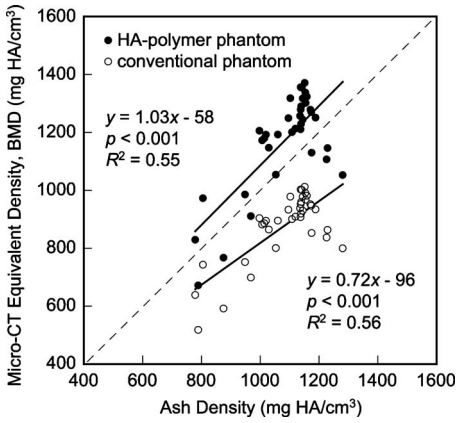

FIG. 4. The BMD of human cortical bone specimens measured by micro-CT equivalent density using the nonlinear calibration for the HA-polymer phantom with an expanded range of HA density was in greater agreement with the corresponding measured ash density (ash mass/TV) compared to using the extrapolated linear calibration for the conventional phantom. The micro-CT equivalent density measured by either calibration was correlated with the measured ash density. Note that measurements of the micro-CT equivalent density using the extrapolated nonlinear calibration for the conventional phantom exhibited only minor differences from the linear calibration (2% greater on average) that were not statistically significant and were therefore not shown for clarity.

IV. DISCUSSION

IV.A. Effects of the calibration phantom composition and imaging medium

The HA-polymer phantom used in this study enabled a more accurate calibration of x-ray attenuation and HA density (Fig. 2), and thus more accurate measurements of BMD and TMD in cortical bone specimens (Figs. 4–6), by virtue of employing (1) an expanded range of HA density

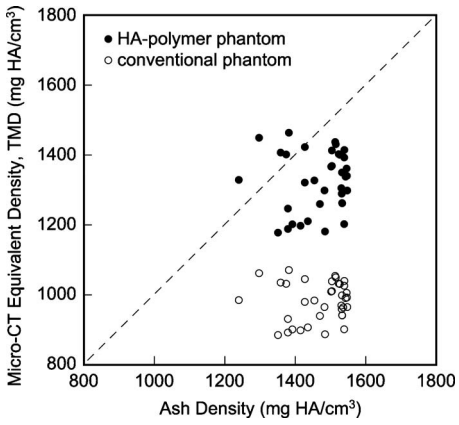

FIG. 5. The TMD of human cortical bone specimens measured by micro-CT equivalent density using the nonlinear calibration for the HA-polymer phantom with an expanded range of HA density was in greater agreement with the corresponding measured ash density (ash mass/BV) compared to using the extrapolated linear calibration for the conventional phantom. The micro-CT equivalent density measured by either calibration was not correlated with the measured ash density. Note that measurements of the micro-CT equivalent density using the extrapolated nonlinear calibration for the conventional phantom exhibited only minor differences from the linear calibration (3% greater on average) that were not statistically significant and were therefore not shown for clarity.

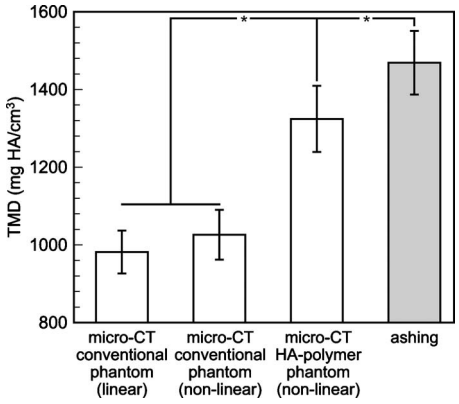

FIG. 6. The mean TMD of human cortical bone specimens measured by micro-CT equivalent density using extrapolated linear or nonlinear calibrations for the conventional phantom, and the nonlinear calibration for the HA-polymer phantom with an expanded range of HA density, compared to the corresponding ash density (ash mass/BV) of the same specimens. Error bars show one standard deviation. Asterisks denote statistically significant differences between groups ($p<0.05$, Tukey's HSD).

(0–1860 mg HA/cm^3) and (2) a less attenuating polymer phase. The range of HA density was inclusive of characteristic levels of BMD in cortical bone or TMD in cortical and trabecular bone. The BMD and TMD of human cortical bone specimens in this study ranged from approximately 700 to 1300 mg HA/cm^3 and from 1200 to 1600 mg HA/cm^3, respectively. However, the conventional calibration phantom included HA density only up to 800 mg HA/cm^3, which may be suitable for the BMD of trabecular bone, but requires extrapolation for levels of BMD observed in cortical bone or levels of TMD in cortical and trabecular bone.

K_2HPO_4 solution phantoms have also been limited to equivalent HA density up to 800–1000 mg HA/cm^3.[16,17,20] Moreover, the solubility limit for K_2HPO_4 in water at 20 °C is 1670 mg/cm^3,[28] which corresponds to ~1600 mg HA/cm^3, depending on imaging parameters. This solubility limit prohibits the preparation of K_2HPO_4 solutions above this concentration and would limit the stability of solutions approaching this concentration. Other recent studies have prepared calibration phantoms comprising ~1200–2000 mg HA/cm^3 by varying the level of porosity in pressed and sintered HA powder compacts.[19,20] However, these phantoms were not able to be prepared at lower mineral density and thus required the use of a second phantom composed of different materials to calibrate HA density below 1200 mg HA/cm^3. Moreover, the air or water in the pore space will not exhibit similar x-ray attenuation to macromolecules like collagen or synthetic polymers. Therefore, a HA-polymer composite phantom is expected to provide greater similarity to the extracellular matrix of bone tissue than liquid K_2HPO_4 or porous HA phantoms.

The HA-polymer phantom in this study utilized HDPE as the polymer phase, whereas the conventional phantom utilized a propriety epoxy resin. The lower density of HDPE (960 mg/cm^3) compared to the epoxy resin (1130 mg/cm^3) resulted in less x-ray attenuation at a fixed HA density, which was evidenced by the vertical shift in calibration curves for the two phantoms even at a HA density of zero (Fig. 2). Polyethylene has also received considerable use for tissue equivalent imaging phantoms.[29]

The imaging medium surrounding phantom or tissue specimens was previously shown to affect the measured x-ray attenuation.[17] In this study, water soaked gauze was used as the imaging medium and was held constant for both the HA-polymer phantom and cortical bone specimens. Furthermore, all phantom and tissue specimens were imaged separately to avoid interference. In contrast, the conventional phantom was comprised of mixtures of HA in an epoxy resin embedded within a single, larger resin block. Moreover, image projections for one HA density were not likely to be completely free from the influence of other HA densities positioned on the opposite side of the phantom (Fig. 3). These effects may have also contributed to the noticeable vertical shift in x-ray attenuation between the two calibration phantoms (Fig. 2). Thus, error due to differences in imaging media was minimized in this study when using the new HA-polymer phantom by scanning all phantom and tissue specimens separately and in the same imaging medium.

IV.B. Effects of the calibration nonlinearity

The relationship between x-ray attenuation and HA density was shown to be nonlinear for the HA-polymer calibration phantom comprising levels of HA density up to 1860 mg HA/cm^3 (Fig. 2). A nonlinear relationship was previously reported for a K_2HPO_4 phantom comprising up to 800 mg HA/cm^3 (Ref. 16) and was reported to slightly improve the calibration correlation coefficient for a pressed and sintered HA phantom comprising 1240–3050 mg HA/cm^3.[19] The results of the present study also showed a slight improvement in the calibration correlation coefficient (Fig. 2) and the accuracy of subsequent BMD and TMD (Fig. 6) measurements in cortical bone specimens when a quadratic rather than a linear relationship was used for the conventional phantom comprising up to 800 mg HA/cm^3. However, a linear relationship was typically expected and employed *a priori* to calibrate measured x-ray attenuation to a known mineral density.[13–20]

The most likely sources for the nonlinear behavior were beam hardening[13–19] and scattering[20,30–32] artifacts, which are dependent on the beam energy spectrum, the attenuation coefficient of the sample, the surrounding media, and the sample geometry. Note that nonlinearity was observed in spite of employing a beam hardening correction algorithm provided by the manufacturer, which is based on a HA-resin wedge phantom with 1200 mg HA/cm^3. This algorithm was previously shown to reduce but not eliminate the effects of beam hardening compared to a 200 mg HA/cm^3 wedge phantom.[13] Thus, the results of this study add further weight to previous evidence that beam hardening due to a polychromatic x-ray source was not able to be fully corrected, especially at high levels of mineralization characteristic of TMD in cortical or trabecular bone.[13–16]

The nonlinear calibration of x-ray attenuation and HA density for the HA-polymer phantom with an expanded

range of HA density was able to compensate for beam hardening artifacts not accounted for by the internal micro-CT correction algorithm, resulting in a more accurate measurement of micro-CT equivalent BMD and TMD in human cortical bone specimens (Figs. 4–6). In practice, the internal calibration provided by the micro-CT manufacturer can be readily corrected by simply applying the nonlinear calibration measured for the HA-polymer phantom with an expanded range of HA density (Fig. 2). For example, the HA density for the new HA-polymer phantom (ρ_{HA}, mg HA/cm^3) was related to the HA density measured using the extrapolated linear calibration for the conventional phantom (ρ_{HA}°) as $\rho_{HA}=(2.89\times10^{-4})\cdot(\rho_{HA}^{\circ})^2+0.97\rho_{HA}^{\circ}+90.63$ ($p<0.001$, $R^2=0.9999$). Note, however, that any calibration relationship must be recognized as being dependent on the instrument, imaging parameters, and specimen size, as has been well-documented.[14–18]

IV.C. Other considerations

The HA-polymer calibration phantom described in this study enabled more accurate measurements of cortical bone mineralization. The micro-CT equivalent TMD of human cortical bone specimens measured using the HA-polymer phantom underestimated the corresponding ash density by 10%, on average (Fig. 6), exhibiting accuracy comparable to previous measurements using SRCT.[13] While encouraging, other factors that may or may not contribute to this error must be considered for further improvement.

Differences in scanning parameters, such as x-ray tube voltage or detector distance, were previously shown to affect x-ray attenuation measurement[17] but were held constant in this study. Moreover, repeated measurements of the conventional calibration phantom provided by the micro-CT manufacturer were in close agreement (Table II), ruling out systematic error. The cross-sectional dimensions of the HA-polymer phantom specimens (10×2.5 mm) were different from those of the cortical bone specimens (5×5 mm), though the cross-sectional area was held constant, which might be expected to result in a different proportion of the cross section influenced by beam hardening compared to the tissue specimens.[15] However, the mean x-ray attenuation of the HA-polymer phantom was not different for a volume of interest at the specimen interior compared to the overall volume, minimizing this concern. Nonetheless, differences in the dimensions of tissue and phantom specimens should always be minimized or calibrated. Beam filtration can also be used to minimize the effects of beam hardening[18] but requires longer image collection times.

The micro-CT equivalent TMD and the corresponding ash density may be subject to error via measurement of the BV, whether using micro-CT (Ref. 13) or Archimedes' principle.[7,25,27] In this study, micro-CT was used by necessity to measure the BV for the equivalent TMD and Archimedes' principle was used to measure the BV for the corresponding ash density, where the latter was regarded as the most accurate assessment of the true tissue porosity. Micro-CT measurements of the tissue porosity were positively correlated with measurements using Archimedes' principle ($p<0.001$, $R^2=0.57$) but were approximately 16.3% lower, on average. An underestimation of tissue porosity by micro-CT was not unexpected due to the resolution limits of the instrument. The use of micro-CT measurements of BV for the corresponding ash density would have resulted in a decreased mean ($\pm$standard deviation) from 1469 ($\pm$80) to 1225($\pm$57) mg HA/cm^3 (cf. Fig. 6), but the latter ash density would not be accurate and would not change the main results of this study. On the other hand, improvements in the accuracy of the BV measured by micro-CT would be expected to lead to decreased BV and consequently increased TMD, improving agreement between the micro-CT equivalent TMD and the corresponding ash density (Figs. 5 and 6). SRCT can be used to improve resolution limits and mitigate the underestimation of BV by micro-CT.[13]

The HA-polymer composite phantom in this study also utilized relatively large HA crystals compared to the size of apatite crystals in bone tissue. The HA crystals exhibited a whiskerlike morphology with mean dimensions of approximately 4–7 μm in length and 2 μm in width.[22] Therefore, while the HA crystal size was smaller than the 10 μm voxel size for the micro-CT instrument, heterogeneity in x-ray attenuation was evident visually, especially at low HA density [Fig. 1(a)], as well as by the measured intrascan spatial variability in x-ray attenuation (Table I). The effect of heterogeneity within phantom specimens was assumed to be minimized by averaging over a relatively large volume of interest, but was not ideal. The use of nanoscale HA crystals in a polymer matrix could provide greater homogeneity to minimize scattering artifacts, similar to K_2HPO_4 solution phantoms,[16,17,20] while retaining the advantages of a HA-polymer phantom mentioned above.

The correlation between the micro-CT equivalent BMD and the corresponding ash density (Fig. 4) was primarily due to variability in BMD caused by the range of porosity included within the TV. In contrast, the lack of a correlation between micro-CT equivalent TMD and the corresponding ash density (Fig. 5) was primarily due to limited variability in TMD resulting from exclusion of tissue porosity in the BV. The addition of other tissue types (e.g., trabecular tissue) and sources (e.g., bovine) could be used to further investigate the correlation of TMD measured by micro-CT and ashing.

V. CONCLUSIONS

A novel HA-polymer composite phantom was prepared comprising a lower attenuating polymer and an expanded range of HA density (0–1860 mg HA/cm^3) inclusive of characteristic levels of BMD in cortical bone or TMD in cortical and trabecular bone. This HA-polymer composite phantom exhibited a nonlinear relationship between x-ray attenuation and HA density, rather than the linear relationship typically employed *a priori*, and obviated the need for extrapolation, when calibrating the measured x-ray attenuation to high levels of mineral density. Therefore, the new HA-polymer phantom resulted in more accurate measure-

ment of micro-CT equivalent BMD and TMD in human cortical bone specimens compared to a conventional phantom, as verified by ash density measurements on the same specimens.

ACKNOWLEDGMENTS

This research was supported by the U.S. Army Medical Research and Materiel Command (Contract No. W81XWH-06-1-0196) through the Peer Reviewed Medical Research Program (Contract No. PR054672) and a Lilly Presidential Fellowship from the University of Notre Dame. The authors thank Andres Laib of Scanco Medical AG for helpful conversations regarding this work.

[a]Author to whom correspondence should be addressed. Electronic mail: rroeder@nd.edu; Telephone: (574) 631-7003; Fax: (574) 631-2144.

[1]P. Ammann and R. Rizzoli, "Bone strength and its determinants," Osteoporosis Int. **14**, S13–S18 (2003).
[2]J. D. Currey, "The effect of porosity and mineral content on Young's modulus of elasticity of compact bone," J. Biomech. **21**(2), 131–139 (1988).
[3]M. B. Schaffler and D. B. Burr, "Stiffness of compact bone: Effects of porosity and density," J. Biomech. **21**(1), 13–16 (1988).
[4]J. Y. Rho, M. C. Hobatho, and R. B. Ashman, "Relations of mechanical properties to density and CT numbers in human bone," Med. Eng. Phys. **17**(5), 347–355 (1995).
[5]C. J. Hernandez, G. S. Beaupré, T. S. Keller, and D. R. Carter, "The influence of bone volume fraction and ash fraction on bone strength and modulus," Bone (Osaka) **29**(1), 74–78 (2001).
[6]O. Akkus, F. Adar, and M. B. Schaffler, "Age-related changes in physicochemical properties of mineral crystals are related to impaired mechanical function of cortical bone," Bone (Osaka) **34**, 443–453 (2004).
[7]J. M. Deuerling, W. Yue, A. A. Espinoza Orías, and R. K. Roeder, "Specimen-specific multiscale model for the anisotropic elastic constants of human cortical bone," J. Biomech. **42**(13), 2061–2067 (2009).
[8]R. D. Bloebaum, J. G. Skedros, E. G. Vajda, K. N. Bachus, and B. R. Constantz, "Determining mineral content variations in bone using backscattered electron imaging," Bone (Osaka) **20**, 485–490 (1997).
[9]P. Roschger, E. P. Paschalis, P. Fratzl, and K. Klaushofer, "Bone mineralization density distribution in health and disease," Bone (Osaka) **42**, 456–466 (2008).
[10]G. Boivin and P. J. Meunier, "The degree of mineralization of bone tissue measured by computerized quantitative contact microradiography," Calcif. Tissue Int. **70**, 503–511 (2002).
[11]C. Schmidt, M. Priemel, T. Kohler, A. Weusten, R. Müller, M. Amling, and F. Eckstein, "Precision and accuracy of peripheral quantitative computed tomography (pQCT) in the mouse skeleton compared with histology and microcomputed tomography (microCT)," J. Bone Miner. Res. **18**, 1486–1496 (2003).
[12]S. Nuzzo, F. Peyrin, P. Cloetens, J. Baruchel, and G. Boivin, "Quantification of the degree of mineralization of bone in three dimensions using synchrotron radiation microtomography," Med. Phys. **29**, 2672–2681 (2002).
[13]G. J. Kazakia, A. J. Burghardt, S. Cheung, and S. Majumdar, "Assessment of bone tissue mineralization by conventional x-ray microcomputed tomography: Comparison with synchrotron radiation microcomputed tomography and ash measurements," Med. Phys. **35**(7), 3170–3179 (2008).
[14]A. J. Burghardt, G. J. Kazakia, A. Laib, and S. Majumdar, "Quantitative assessment of bone tissue mineralization with polychromatic micro-computed tomography," Calcif. Tissue Int. **83**, 129–138 (2008).
[15]R. J. Fajardo, E. Cory, N. D. Patel, A. Nazarian, A. Laib, R. K. Manoharan, J. E. Schmitz, J. M. DeSilva, L. M. MacLatchy, B. D. Snyder, and M. L. Bouxsein, "Specimen size and porosity can introduce error into μCT-base tissue mineral density measurements," Bone (Osaka) **44**, 176–184 (2009).
[16]L. Mulder, J. H. Koolstra, and T. M. G. J. Van Eijden, "Accuracy of microCT in the quantitative determination of the degree and distribution of mineralization in developing bone," Acta Radiol. **45**(7), 769–777 (2004).
[17]A. Nazarian, B. D. Snyder, D. Zurakowski, and R. Müller, "Quantitative micro-computed tomography: A non-invasive method to assess equivalent bone mineral density," Bone (Osaka) **43**, 302–311 (2008).
[18]J. A. Meganck, K. M. Kozloff, M. M. Thornton, S. M. Broski, and S. A. Goldstein, "Beam hardening artifacts in micro-computed tomography scanning can be reduced by x-ray beam filtration and the resulting images can be used to accurately measure BMD," Bone (Osaka) **45**, 1104–1116 (2009).
[19]S. Schweizer, B. Hattendorf, P. Schneider, B. Aeschlimann, L. Gaukler, R. Müller, and D. Günther, "Preparation and characterization of calibration standards for bone density determination by micro-computed tomography," Analyst (Cambridge, U.K.) **132**, 1040–1045 (2007).
[20]W. Zou, J. Gao, A. S. Jones, N. Hunter, and M. V. Swain, "Characterization of a novel calibration method for mineral density determination of dentine by x-ray micro-tomography," Analyst (Cambridge, U.K.) **134**, 72–79 (2009).
[21]R. K. Roeder, M. S. Sproul, and C. H. Turner, "Hydroxyapatite whiskers provide improved mechanical properties in reinforced polymer composites," J. Biomed. Mater. Res. **67A**(3), 801–812 (2003).
[22]W. Yue and R. K. Roeder, "Micromechanical model for hydroxyapatite whisker reinforced polymer biocomposites," J. Mater. Res. **21**(8), 2136–2145 (2006).
[23]W. Suchanek, H. Sada, M. Yashimi, M. Kakihana, and M. Yoshimura, "Biocompatible whiskers with controlled morphology and stoichiometry," J. Mater. Res. **10**(3), 521–529 (1995).
[24]Powder Diffraction File Card No. 09-0432, $Ca_5(PO_4)_3OH$, hydroxylapatite (JCPDS–International Center for Diffraction Data, Newton Square, PA, 1997).
[25]ASTM Standard C 373-88, "Standard test method for water absorption, bulk density, apparent porosity, and apparent specific gravity of fired whiteware products" (American Society for Testing and Materials, West Conshohocken, PA, 1999), pp. 119–120.
[26]R. B. Ashman, S. C. Cowin, W. C. Van Buskirk, and J. C. Rice, "A continuous wave technique for the measurement of the elastic properties of cortical bone," J. Biomech. **17**(5), 349–361 (1984).
[27]X. Wang, R. A. Bank, J. M. TeKoppele, and C. M. Agrawal, "The role of collagen in determining bone mechanical properties," J. Orthop. Res. **19**, 1021–1026 (2001).
[28]*CRC Handbook of Chemistry and Physics*, edited by D. R. Lide (CRC, Boca Raton, FL, 1993), pp. 4–88.
[29]W. A. Kalender and C. Suess, "A new calibration phantom for quantitative computed tomography," Med. Phys. **14**(5), 863–866 (1987).
[30]S. Prevrhal, K. Engelke, and W. A. Kalender, "Accuracy limits for the determination of cortical width and density: The influence of object size and CT imaging parameters," Phys. Med. Biol. **44**, 751–764 (1999).
[31]J. H. Siewerdsen, M. J. Daly, B. Bakhtiar, D. J. Mosely, S. Richard, H. Keller, and D. A. Jaffray, "A simple, direct method for x-ray scatter estimation and correction in digital radiography and cone-beam CT," Med. Phys. **33**, 187–197 (2006).
[32]J. S. Bauer, T. M. Link, A. Burghardt, T. D. Henning, D. Mueller, S. Majumdar, and S. Prevrhal, "Analysis of trabecular bone structure with multidetector spiral computed tomography in a simulated soft-tissue environment," Calcif. Tissue Int. **80**, 366–373 (2007).